PHYSICAL REVIEW C VOLUME 27, NUMBER 2 FEBRUARY 1983

Pion-nucleus forward scattering amplitudes from total cross section measurements

R. H. Jeppesen and M. J. Jakobson
University of Montana, Missoula, Montana 59812

M. D. Cooper, D. C. Hagerman, M. B. Johnson, and R. P. Redwine*
Los Alamos National Laboratory, Los Alamos, New Mexico 87545

G. R. Burleson and K. F. Johnson†
New Mexico State University, Las Cruces, New Mexico 88003

R. E. Marrs‡
California Institute of Technology, Pasadena, California 91109

H. O. Meyer§
University of Basel, Basel, Switzerland

I. Halpern
University of Washington, Seattle, Washington 98195

L. D. Knutson
University of Wisconsin, Madison, Wisconsin 53706
(Received 9 September 1982)

Measurements have been made of the attenuation cross sections for both π^+ and π^- mesons on Al, ^{40}Ca, Cu, Sn, Ho, and Pb nuclei. The measurements were made at several energies between 114 and 215 MeV. A new method of data analysis has been used to extract both the real and the imaginary parts of a Coulomb-distorted forward scattering amplitude $f_N(0)$. Insight into the nature of $f_N(0)$ is obtained by the comparison of experimental data with theoretical values calculated from a simple absorption model. This comparison demonstrates that much of the observed rotation of the forward amplitude, when plotted on an Argand diagram, can be attributed to the Coulomb phase contained in $f_N(0)$. Comparison is also made with results of similar experiments. Although the present results are in general agreement with previously published ones, some differences are noted for the heavier elements.

[NUCLEAR REACTIONS Measured pion forward scattering amplitudes; Al, ^{40}Ca, Cu, Sn, Ho, and Pb; $E=114$–215 MeV; strong absorption model.]

I. INTRODUCTION

Traditionally, measurements of the total cross section σ_T have been among the first experiments to be made in any new systematic study of hadronic interactions with matter. In pion physics, it has been expected that accurate pion-nucleus total cross sections would be useful for studying the neutron halo as a function of N and Z.[1] Furthermore, knowledge of σ_T gives directly the imaginary part of the forward scattering amplitude. This is needed for determination of the real part of the forward scattering amplitude experimentally through Coulomb-nuclear interference measurements[2] or theoretically through dispersion relations.[3] Knowledge of both the real and imaginary parts is necessary for optical model calculations. The comparison of different reaction models requires more information than is available from precise elastic measurements alone.[4] We have made a set of pion attenuation measurements with both π^+ and π^- mesons on various nuclei including Al, Ca, Cu, Sn, Ho, and Pb. Here we report the experimental results on these nuclei in the laboratory energy range of 114 to 215 MeV and give a qualita-

tive interpretation of them.

The experiment is described in Sec. II. It is emphasized there that for pion-nucleus scattering in this energy range the analysis of the experimental data is complicated by two factors; first, by the large model-dependent Coulomb multiple scattering corrections which are necessary at small angles and second, by the significant Coulomb-nuclear interference which occurs at the larger angles where the multiple scattering corrections are manageable. These difficulties are enhanced by the large Z of the nuclear targets.

We have relied on the methods of Ref. 5 for extrapolating the experimental results to small angles. Reference 5 shows that the quantity which may be obtained in a model-independent fashion (in principle) is $f_N(0)$, where $f_N(\Omega)$ is defined as

$$f_N(\Omega) \equiv F(\Omega) - f_C(\Omega) . \tag{1}$$

Here $F(\Omega)$ is the total elastic scattering amplitude and $f_C(\Omega)$ is the relativistic point Coulomb amplitude. The details of the method used for the extrapolation are discussed in Sec. III.

The quantity reported in this paper is $f_N(0)$. The results are given in Sec. IV. This quantity is different from the purely strong amplitude which is related to σ_T by the standard optical theorem.[6] However, $f_N(0)$ is a useful physical quantity because it is calculable by standard optical model computer programs and can be related directly to Coulomb-nucleus interference measurements. For large Z we obtain both the real and imaginary part of f_N from the attenuation measurement. Correcting these quantities for Coulomb effects should enable one to determine σ_T as well as the real part of the purely strong forward scattering amplitude for comparison with the results of forward dispersion calculations. For small Z, Coulomb corrections can be made by elementary Bethe phase analysis.[7] For Z large, the Coulomb interaction is so strongly mixed with the strong interaction that the Bethe phase analysis is of questionable utility. A simple interpretation of our results is given in Sec. V in terms of a strong absorption model. Comparison of our results with other experiments is made in Sec. VI and the final summarization is made in Sec. VII.

II. EXPERIMENTAL DETAILS

These measurements are part of a larger research effort directed towards the measurement of pion-nucleus attenuation cross sections for a number of nuclei ranging from He to Pb. The experiment was done at LAMPF using the low-energy pion channel (LEP) (Ref. 8) which provides a beam with good energy resolution and small divergence, π^+ or π^- energies of 20 to 300 MeV, sufficient isochronism to preserve the microtime structure of the beam for time-of-flight measurements, and a relatively small beam spot (~ 1.5 cm diameter).

A. Experimental setup

The setup was that of a standard attenuation measurement. The fraction of the incident beam scattered into a given solid angle was measured by a stack of concentric cylindrical scintillation counters of increasing radii located downstream of the target. If the solid angle subtended at the target by the ith counter is Ω_i, the partial cross section for removal from the incident beam, $\sigma(\Omega_i)$, is given by

$$\sigma(\Omega_i) = \frac{1}{nt} \ln \frac{R_0(\Omega_i)}{R(\Omega_i)} , \tag{2}$$

where $R(\Omega_i)$ is the fraction of the incident beam detected by the counter with target in place and $R_0(\Omega_i)$ is the result of an analogous measurement using an empty target. The number of target nuclei per unit volume is given by n and the thickness of the target by t. The forward amplitude is found by a suitable extrapolation of the $\sigma(\Omega_i)$ to zero solid angle, as discussed below.

Beam pion identification was made by a differential isochronous self-collimating Cherenkov (DISC) counter[9] at energies above 100 MeV. Time-of-flight techniques[10] were used at lower energies. A set of three multiwire proportional chambers provided information concerning the profile of the beam upstream of the target. A schematic diagram of the experimental setup is shown in Fig. 1. General information concerning this type of attenuation measurement can be found in Ref. 11.

B. Special design consideration

Special consideration was given during the design of the experiment to problems that could be encoun-

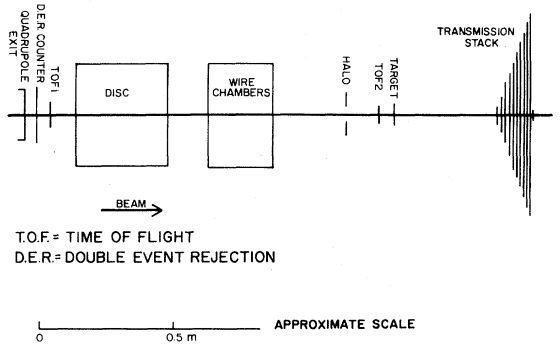

FIG. 1. Schematic diagram of experimental setup.

tered because of high counting rates or changes in beam intensity. Electronic logic was used to make corrections for accidental events in the transmission counters, for pion absorption in these counters, and for counter efficiency.

In order to reduce the size of the accidental correction which is associated with the high counting rates in the larger transmission counters, a double-event rejection system was used. A scintillation counter positioned ahead of the experiment detected all beam particles. A particle passing through this counter would open a "time gate" of approximately 50 ns in length. If a second particle passed through the counter during the time that the gate was open, both events were rejected. Rejection of events in which two or more particles passed through the system at close to the same time was accomplished by cuts on pulse height.

Any systematic error due to variations in beam intensity between target-in and target-out runs was averaged by the frequent cycling of targets. The targets used in the experiment were cylindrical in shape with a diameter of approximately 38 mm and a thickness given in Table I. The targets were placed in holders mounted on a multipositioned target wheel capable of holding up to eight different targets. During each run, the target wheel position was changed at roughly two minute intervals to average out fluctuations and drifts in beam intensity when comparing targets. Care was taken during the fabrication of the targets and the target holders to ensure that all targets used during a single run, including the empty target, would be identical as far as the target support mechanism was concerned. A PDP-11 computer was used on line for data taking and target cycling. Some details of the experimental setup have been included in other reports.[12,13]

C. Multiple scattering and decay corrections

The quantity of direct interest in this experiment was the number of pions scattered into the angular region defined by each of the transmission counters located downstream of the target. The events for each counter were scaled as were events used to determine the corrections due to accidental counts, counter efficiency, and absorption of pions in the transmission counters. After making such corrections, scalar readings for target-in and target-out measurements were used to obtain a partial cross section for each counter according to Eq. (2). A Monte Carlo simulation[14] was then used to make corrections for effects, described below, whose magnitude could not be determined directly from scalar readings. The simulation corrections proved to be substantial for high Z targets. For example, this correction amounted to 61% of the partial cross section as measured by the innermost counter, $T1$, for π^+ pions on lead at 115 MeV. For counter $T2$, the correction was substantially less than for $T1$, amounting to 33% of the partial cross section for π^+ pions on lead at 115 MeV. Because of the large correction, counter $T1$ was not used to extract $f_N(0)$ but instead was only used for a check of the extrapolation procedure.

The Monte Carlo simulation was used to make corrections for the following:

(1) decay of pions both upstream and downstream of the target;
(2) finite beam size and divergence and finite target size;
(3) straggling in the target;
(4) multiple Coulomb scattering in the target, the upstream counters, and the wire chambers;
(5) nuclear scattering and pion removal by interaction in the upstream counters;
(6) absorption of pions by the light pipes;
(7) multiple scattering of muons from pion decay upstream of the target;
(8) energy loss of muons from upstream decay in the target, time-of-flight counter, and the light pipes.

The Monte Carlo decay and multiple scattering corrections were checked experimentally by beam profile comparisons and target thickness comparisons.

In addition, the extracted data were subjected to several constraints. (1) The "beam" profile generated by the Monte Carlo program had to be in agreement with the measured beam profile obtained by use of multiwire proportional chambers upstream of the target. (2) Since the outer counters were less affected by the effects simulated using the Monte Carlo code, we required that the forward scattering amplitude obtained by means of a least squares fit using the nine outer counters of the transmission stack should agree, within statistics, with the forward scattering amplitude obtained using the eight outer

TABLE I. Targets used in this experiment.

Target	Thickness (g/cm^2)
Al	0.968
^{40}Ca	1.510
Cu	1.159
Sn	1.429
Ho	0.928
Pb	0.871

counters of the transmission stack. When fewer than nine counters were used, the same constraint was applied using the smaller number of counters. (3) Runs made with similar beam tunes were required to have similar input parameters for the Monte Carlo code. (4) Corrections obtained by use of the Monte Carlo code had to give values of $f_N(0)$ which varied smoothly with energy since theoretical calculations using PIRK (Ref. 15) indicated that $f_N(0)$ has this property. (5) These corrections also had to bring the partial cross section corresponding to the first counter in the stack in general agreement with the partial cross sections corresponding to the other counters. This was assumed to have been done if the partial cross section for the first counter, extrapolated by a fit to the partial cross sections for the other counters, agreed within one or two standard deviations of the measured value for the first counter. There was some variation in the degree to which the constraints were satisfied. In general, these constraints were more difficult to satisfy for the π^+ runs.

III. THEORY

If the corrected partial cross section, $\sigma(\Omega_i)$, were a sufficiently smooth function of Ω near $\Omega=0$, it would be possible to obtain $\sigma(0)$ by extrapolation of $\sigma(\Omega)$ to zero solid angle. It is in this way that one, for example, measures $\sigma(0)$ for neutrons. For experiments with charged projectiles, the direct extrapolation of the measured partial cross section is complicated by Coulomb effects unless the measurement of $\sigma(\Omega_i)$ is confined to solid angles for which the Coulomb interaction is negligible. In practice, direct extrapolation is possible only in high energy experiments or low-Z experiments such as p-p scattering. For other experiments, the Coulomb interaction must be taken into consideration. Usually this is done by the subtraction of all terms containing the Coulomb scattering amplitude from the corrected transmission data. Extrapolation of this partial cross section $\sigma_R(\Omega)$ to $\Omega=0$ gives what has been referred to as the removal or total cross section. A difficulty with this method is the need for a nuclear model to remove the Coulomb-nuclear interference term from the measured partial cross section. As a result, the partial cross sections are inherently model dependent. Previous measurements have shown that this can be significant for pions on nuclei as low in Z as carbon at energies up to 280 MeV.[16]

To alleviate these difficulties for heavy targets and low bombarding energies, the Coulomb singularity was removed from the corrected cross section data by subtracting only the contribution due to pure Coulomb scattering according to the following prescription:

$$\sigma_N(\Omega)=\sigma(\Omega)-\int_\Omega^{4\pi}|f_C|^2 d\Omega' . \tag{3}$$

Because of the Coulomb-nuclear interference, $\sigma_N(\Omega)$ oscillates with increasing frequency as $\Omega\to 0$. This behavior precludes the possibility of obtaining $\sigma_N(0)$ by fitting with a polynomial form.[5] Instead, $\sigma_N(\Omega)$ is parametrized with an analytic expression which contains the real and the imaginary parts of $f_N(0)$ as adjustable parameters. Values of these parameters are obtained from a least squares fit to the data.

The procedure used to obtain a parametrized expression for $\sigma_N(\Omega)$ follows the method which was developed by Cooper and Johnson[5] with the addition of the relativistically correct expression for the Coulomb amplitude $f_C(\Omega)$ developed in Ref. 17. Since the basic theory is developed in Ref. 5, we include only the results of the derivation in this section. Some additional details on the derivation are to be found in the Appendix.

The Coulomb-distorted cross section, $\sigma_N(\Omega)$, is related to the scattering amplitude, $f_N(\Omega)$, and the relativistic point Coulomb amplitude, $f_C(\Omega)$, by

$$\sigma_N(\Omega)=\sigma_a(\Omega)+\int_\Omega^{4\pi}|f_N|^2 d\Omega' + 2\,\mathrm{Re}\int_\Omega^{4\pi} f_C^* f_N d\Omega' , \tag{4}$$

where the reaction (or absorption) cross section $\sigma_a(\Omega)$ is defined according to

$$\sigma_a(\Omega)=\sigma(\Omega)-\int_\Omega^{4\pi}\frac{d\sigma_{\mathrm{el}}}{d\Omega'}d\Omega' . \tag{5}$$

If one assumes a power series expansion for both $f_N(\Omega)$ and $\sigma_a(\Omega)$ about $\Omega=0$, then

$$\sigma_N(\Omega)=\frac{4\pi}{k}f_N^I G(\Omega)+\frac{4\pi}{k}f_N^R H(\Omega)+\sum_{n=1} K_n\Omega^n + \sum_{n=0} B_n\Omega^{(n/2)+1}\cos W + \sum_{n=0} C_n\Omega^{(n/2)+1}\sin W , \tag{6}$$

where

$$f_N^I=\mathrm{Im}f_N(0) ,$$

$$f_N^R=\mathrm{Re}f_N(0) ,$$

and

$$W=\eta\ln(\Omega/4\pi)-2\sigma_0$$

with η and σ_0 as defined in Ref. 17. Both $G(\Omega)$ and $H(\Omega)$ are known functions of Ω. K_n, B_n, and C_n are adjustable parameters.

The number of parameters needed to fit the data

can be reduced by using an optical model potential to obtain theoretical values of $\sigma_N(\Omega)$. Then the difference between the experimental and theoretical values of the cross section is fitted to the following equation:

$$\delta\sigma(\Omega)\equiv\sigma(\Omega)-\sigma_T(\Omega)$$
$$=\frac{4\pi}{k}\delta f_N^I G(\Omega)+\frac{4\pi}{k}\delta f_N^R H(\Omega)+\sum_{n=1} K_n'\Omega^n$$
$$+\sum_{n=0} B_n'\Omega^{(n/2)+1}\cos W$$
$$+\sum_{n=0} C_n'\Omega^{(n/2)+1}\sin W\ . \tag{7}$$

The adjustable parameters δf_N^R and δf_N^I are the real and the imaginary parts, respectively, of the differences between the extrapolated and the theoretical values of the forward scattering amplitude. Since the optical model serves only to change the adjustable parameters between Eqs. (6) and (7), this technique has been called the indirect method in Ref. 5. We use the same notation. If the model reproduces the higher-order terms reasonably well, fewer terms will be needed to obtain an acceptable fit to the data than would be the case if Eq. (6) were used. With this assumption, it was possible to obtain a reasonable fit to the data (as measured by a reduced chi-squared distribution) using the four parameter equation given by

$$\delta\sigma_N(\Omega)=\frac{4\pi}{k}\delta f_N^I G(\Omega)+\frac{4\pi}{k}\delta f_N^R H(\Omega)$$
$$+K_1'\Omega+K_2'\Omega^2\ , \tag{8}$$

where the fitted parameters are $(4\pi/k)\delta f_N^I$, $(4\pi/k)\delta f_N^R$, K_1', and K_2'. Equation (7) remains independent, in principle, of the details of the model used in the fit. Whether or not this is true for results which are obtained by use of Eq. (8) is dependent upon the contribution of the higher-order terms which have been dropped from Eq. (7). In this analysis both the Kisslinger[18] and the local Laplacian[19] models were used. As will be shown in the next section, comparison of the results obtained by these two models indicates that any systematic error due to model dependence is within the statistical uncertainties of the experiment.

IV. RESULTS

Results of the calculations summarized in the previous section are tabulated in Table II. The values represent the average of using Kisslinger and local Laplacian models to calculate the higher order terms. These models have quite different off-mass-shell momentum extrapolations. The magnitude of the difference between the two sets of extrapolated amplitudes is also given in Table II. Figures 2–5 display the Z dependence of $(4\pi/k)f_N(0)$ for each of the energies covered in this paper. The partial cross sections which were used to extract the above information have been tabulated and are available from the authors.

The error listed for each of the experimental values of $(4\pi/k)f_N(0)$ is not entirely statistical in nature. It includes a factor which represents the uncertainty associated with the description of the pion beam used in the Monte Carlo calculations. In the data analysis for the experiment, several Monte Carlo calculations were made in which the input parameters were varied slightly. The results of those tests indicated that the actual uncertainty in the results should be somewhat greater than that represented by statistical errors alone. In order to take this into consideration, there was added the constraint that the reduced chi-squared distribution for the data as a whole had to be in agreement with theoretical distributions.[20] We found that this constraint was satisfied if the size of the error bars for the partial cross section was increased by 15%. This error bar increase was in agreement with the tests that were run on the Monte Carlo code.

The presence of higher order terms in Eq. (7) makes it unlikely that results obtained by use of Eq. (8) and the Kisslinger model would be exactly the same as those obtained by use of Eq. (8) and the local Laplacian model. When plotted on an Argand diagram, it was found that the agreement between values of $(4\pi/k)f_N(0)$ obtained by the two methods is quite good. However, there does appear to be some systematic effect in the difference between them. In order to determine the magnitude of any systematic error due to model dependence, the quantity

$$\Delta F=f_N^K(0)-f_N^L(0) \tag{9}$$

was evaluated for both theoretical and experimental values of $f_N(0)$. In this expression $f_N^K(0)$ is the value obtained for $f_N(0)$ using the indirect method and the Kisslinger model while $f_N^L(0)$ is the corresponding value obtained with the use of the local Laplacian model. In polar notation, ΔF corresponds to a vector drawn from the data point associated with $f_N^L(0)$ to the data point associated with $f_N^K(0)$. If there were no model dependence, one would expect the experimental values of ΔF to have a magnitude which was consistent with zero and an argument which would have random values. The results for ΔF indicate that there is some residual model dependence in the method which was used to extract $f_N(0)$. The experimental values of the magnitude of ΔF are essentially statistically equal to zero; the values for

TABLE II. $(4\pi/k)f_N(0)$ for π^+ and π^- mesons. The quantities reported in this table represent the average value of the forward scattering amplitude obtained by use of the indirect method with the Kisslinger and local Laplacian models. The column labeled $(4\pi/k)\,|\Delta F|$ gives the magnitude of the difference of the results which were obtained using the two models.

	π^+			π^-		
Energy (MeV)	Real $\frac{4\pi}{k}f_N(0)$ (mb)	Imag $\frac{4\pi}{k}f_N(0)$ (mb)	$\frac{4\pi}{k}\lvert\Delta F\rvert$ (mb)	Real $\frac{4\pi}{k}f_N(0)$ (mb)	Imag $\frac{4\pi}{k}f_N(0)$ (mb)	$\frac{4\pi}{k}\lvert\Delta F\rvert$ (mb)
Aluminum						
114.5	−111±243	1038±114	156	675±308	1032±143	150
140.0	157±239	1263±112	210			
164.9	−547±223	952±107	149	230±222	1207±104	119
215.3	−933±196	699±99	51	150±208	1118±103	29
Calcium						
114.0	−336±163	1454±126	297	1067±176	1209±135	228
139.5	−453±173	1452±135	245	984±141	1232±110	164
164.5	−634±159	1299±127	173	364±142	1656±114	96
189.7	−693±141	1262±116	120	260±109	1676±89	48
214.8	−934±108	990±93	73	315±99	1583±83	16
Copper						
114.5	−917±131	1558±196	343	1504±198	1519±280	258
139.9	−963±133	1706±192	340			
164.9	−1290±120	1217±181	230	1291±129	1797±185	112
215.2	−1376±99	973±165	89	1228±103	1581±163	12
Tin						
114.4	−2424±46	1235±204	464	3004±47	869±255	102
139.9	−2539±43	665±216	363			
164.8	−2435±43	167±188	241	3086±40	423±193	58
215.2	−2172±51	−522±166	115	3025±42	551±163	76
Holmium						
140.3	−2356±212	−1442±242	318			
165.2	−2127±306	−1995±306	223	3726±300	−1224±367	140
215.5	−1793±229	−1952±181	121	3809±208	−1371±196	111
Lead						
114.9	−1798±289	−2476±104	448	2023±316	−3576±155	272
140.3	−1059±418	−2751±130	308			
165.3	−261±381	−2790±108	209	2057±368	−3671±146	160
215.6	494±354	−2737±86	122	1980±325	−3624±92	118

the argument are not random.

V. INTERPRETATION OF DATA

A. Bethe phase calculations

Theoretical investigations between the purely strong amplitude $f_s^{\pm}(0)$ and $f_N(0)$ have been done by numerous investigators.[7,21,22] If $f'_N(0)$ is defined to be the forward nuclear amplitude obtained from Eq. (1) by replacing $f_C(0)$ with the Coulomb amplitude for an extended charge distribution, then

$$f'^{\pm}_N(0)=e^{i\phi_B^{\pm}(0)}f_s^{\pm}(0)\,, \tag{10}$$

where $\phi_B^{\pm}(0)$ is the Bethe phase. It has previously been shown[7] that $f'_N(0)$ is approximately related to $f_N(0)$ by

$$f'_N(0)=f_N(0)-\tfrac{1}{3}\eta kR_c^{\,2}\,, \tag{11}$$

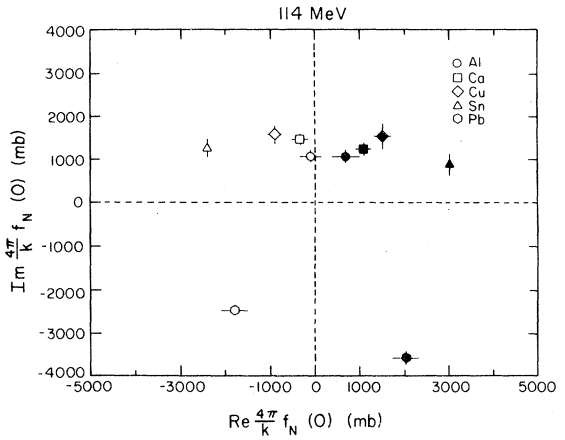

FIG. 2. $(4\pi/k)f_N(0)$ for 114 MeV pions. Data points corresponding to π^+ scattering are represented by open symbols while those for π^- scattering are represented by closed symbols.

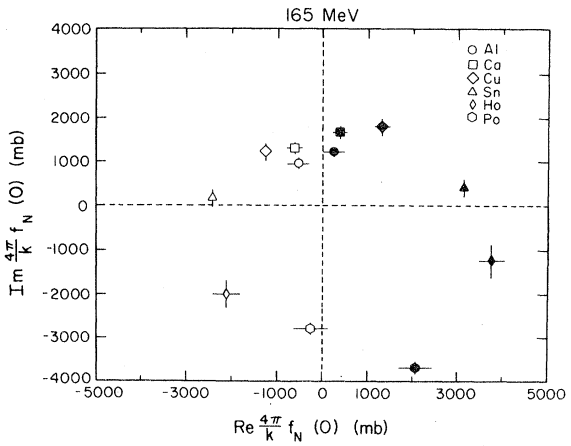

FIG. 4. $(4\pi/k)f_N(0)$ for 165 MeV pions. Data points corresponding to π^+ scattering are represented by open symbols while those for π^- scattering are represented by closed symbols.

where R_c^2 is the sum of the squares of the pion and nucleus root-mean-square charge radii. For $N=Z$ nuclei[7]

$$f_s(0)=f_s^+(0)=f_s^-(0)$$
$$=[f_N'^+(0)f_N'^-(0)]^{1/2} \quad (12a)$$

and

$$\phi_B(0)=\phi_B^+(0)=-\phi_B^-(0)$$
$$=-i\ln[f_N'^+(0)/f_s(0)]\,. \quad (12b)$$

In the results reported here, ^{40}Ca is the only nucleus for which $N=Z$. The applications of Eqs. (11), (12a), and (12b) to the forward scattering amplitudes give the values for $f_s(0)$ and $\phi_B(0)$ displayed in Figs. 6 and 7, respectively. Figure 6 also contains a result found for 180 MeV pions on ^{40}Ca by Germond and Johnson[23] from elastic scattering data. Theoretical values of $\phi_B(0)$ have also been obtained by Cooper, Johnson, and West. As can be seen in Fig. 7, our measurements for the imaginary part of $\phi_B(0)$ are in agreement with theory while those for the real part differ by about one standard deviation.

The energy for which the real part of $f_s(0)$ is zero is of interest since that energy can be defined to be the resonance energy for the pion-nucleus interaction. An estimate of the resonance energy for ^{40}Ca is made by means of a straight-line fit to the data and is found to be

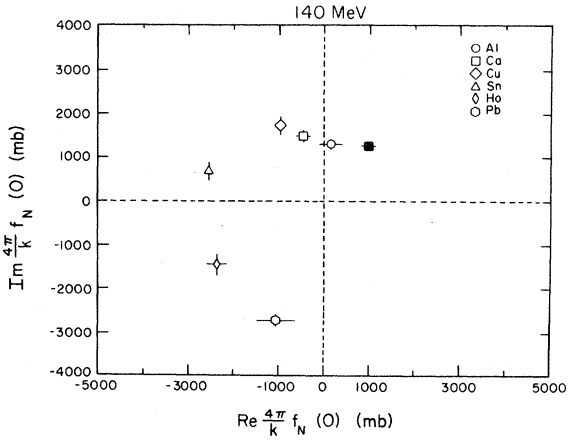

FIG. 3. $(4\pi/k)f_N(0)$ for 140 MeV pions. Data points corresponding to π^+ scattering are represented by open symbols while those for π^- scattering are represented by closed symbols.

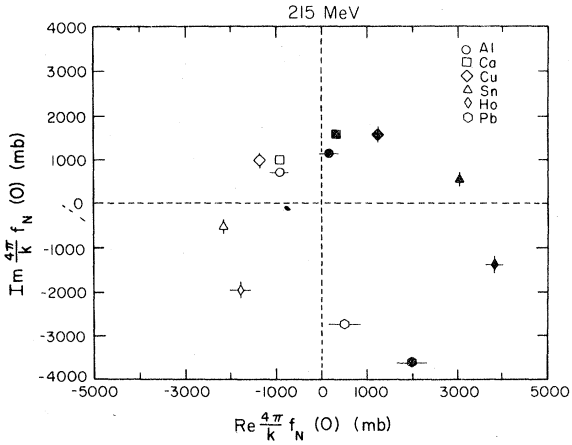

FIG. 5. $(4\pi/k)f_N(0)$ for 215 MeV pions. Data points corresponding to π^+ scattering are represented by open symbols while those for π^- scattering are represented by closed symbols.

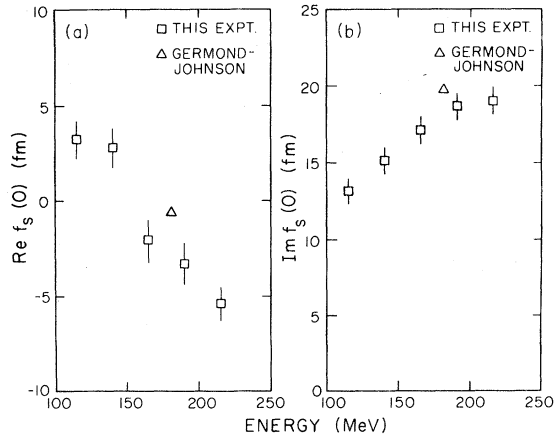

FIG. 6. Real and imaginary parts of the purely strong forward amplitude for pions on ^{40}Ca.

$$T_\pi = 154 \pm 10 \text{ MeV} . \tag{13}$$

This may be compared to results of a similar calculation by Cooper, Johnson, and West on ^{16}O.[7] There $\mathrm{Re}f_s(0)$ was found to be zero for $T_\pi = 178 \pm 4$ MeV. The lower resonance energy observed in this experiment for ^{40}Ca is consistent with a trend observed by Albanese *et al.*[4] They evaluate elastic scattering data using the method of complex zeros and find $\mathrm{Im}q_1^{\,2}$ to be zero at 163 MeV for ^{16}O as opposed to 180 MeV for ^{12}C and 210 MeV for ^{4}He. Germond and Wilkin show that $\mathrm{Im}q_1^{\,2}$ is directly related to $\mathrm{Re}f_s(0)$ if one assumes a simple strong absorption model which may be good near resonance.[24] Hence one would expect the same energy dependence for $\mathrm{Re}f_s(0)$ as has been reported for $\mathrm{Im}q_1^{\,2}$.

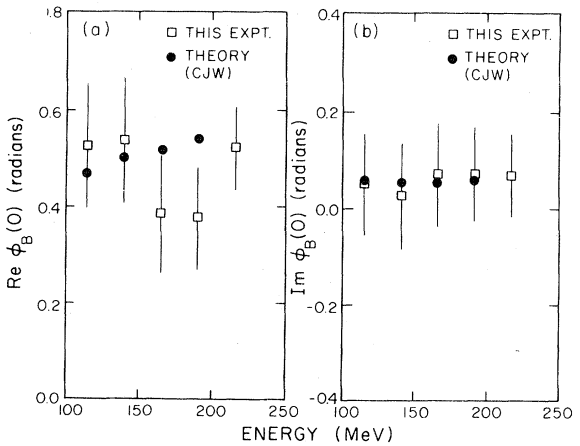

FIG. 7. Real and imaginary parts of the Bethe phase for pions on ^{40}Ca.

B. Absorption model calculations

The dependence of the experimentally determined $f_N(0)$ on Z and energy is displayed in the Argand diagrams of Figs. 2–5. For high Z elements, this amplitude differs substantially from the purely strong amplitude $f_s(0)$ which is related to the total cross section by the usual optical theorem. The behavior of $f_N(0)$ is determined by both the strong and Coulomb forces. At a quantitative level these two forces are highly mixed and an optical model analysis is required in order to extract the new information which is contained in the data. However, the dominant trends in the data, for example, the negative value of $\mathrm{Im}f_N(0)$ for heavy nuclei such as lead and holmium, can be understood in an elementary strong absorption model.

In this model the eikonal approximation is used.[25] The partial wave expansion for $f_N(0)$ is written as an integral over the impact parameter b.

$$f_N(0) = \frac{k}{i} \int_0^\infty b\, db\, e^{2i\sigma_\gamma} [\xi(b) e^{2i\delta'(b)} - 1] . \tag{14}$$

The phase shift $\delta'(b)$ and the absorption coefficient $\xi(b)$ are real. The Coulomb interaction V_C is contained in σ_γ (the relativistic Coulomb phase shift) defined according to

$$e^{2i\sigma_\gamma} = e^{-i\pi[\gamma - l - (1/2)]} \frac{\Gamma(\gamma + \frac{1}{2} + i\eta)}{\Gamma(\gamma + \frac{1}{2} - i\eta)} , \tag{15a}$$

$$\gamma^2 = (l + \tfrac{1}{2})^2 - Z^2\alpha^2, \quad l \simeq kb + \tfrac{1}{2} . \tag{15b}$$

Since the scattering occurs near the (3,3) resonance, one can choose

$$\xi(b) = \frac{1}{1 + e^{-[(b-c)/a]}} \tag{16a}$$

and

$$\delta'(b) = 0 , \tag{16b}$$

where the half radius c is corrected for the Coulomb trajectory distortion of the pion.[26] In a lowest order optical potential description, the parameters c and a can be related to the nuclear density distribution $\rho(r)$ near the point where $\rho(r=c)/\rho(r=0) \simeq 0.1$.[27] A crude parametrization of the results described in Ref. 27 gives

$$c \simeq 1.4A^{1/3} \text{ fm} + \frac{\eta}{k} , \tag{17a}$$

$$a \simeq 0.65 \text{ fm} . \tag{17b}$$

Effects arising from the finite extent of the charge distribution and the real part of the optical potential are ignored in the approximation in Eq. (16b). The extent to which $\delta'(b)$ differs from zero is discussed

below.

The effect of the Coulomb amplitude in the model of Eqs. (14) and (16) is shown in Fig. 8. If $\sigma_\gamma=0$, $f_N(0)$ is purely imaginary and all points will lie along the imaginary axis. This case is represented by the dotted line in Fig. 8. In the case $\sigma_\gamma=0$, one observes that the calculated values of the forward scattering amplitudes are the same for π^+ and π^- mesons. For nuclei with a neutron excess, this degeneracy would be broken by the strong interaction, but it does not occur here because of the simple approximations used. Introduction of the Coulomb phase, according to Eq. (15), also removes the degeneracy, as shown by the dashed curve. Besides undergoing a small change in magnitude, the calculated values of $f_N(0)$ undergo a rotation in the Argand diagrams. The rotation is clockwise for π^- mesons and counterclockwise for π^+ mesons. The degree of rotation is observed to increase with increasing Z. In the particular cases of Pb and Ho, the rotation is large enough to make the imaginary part of the scattering amplitudes negative.

The difference between the data and simple theory is largest for the higher-Z nuclei. Examination of the difference reveals that the rotation due to the Coulomb phase is too large for π^- and too small for π^+ mesons. Because 165 MeV is not exactly the resonance energy, we are led to consider that our assumption $\delta'(b)=0$ may be the source of this discrepancy. If $\delta'(b)$ in Eq. (14) is small we find

$$f_N(0)\rightarrow f_N(0,\delta')=e^{i\Phi}f_N(0)\,, \tag{18a}$$

$$\Phi\simeq 2\frac{\int_0^\infty b\,db\,\delta'(b)\xi(b)}{\int_0^\infty b\,db[\xi(b)-1]}\,. \tag{18b}$$

Rather than calculate Φ from the eikonal model, it is evaluated from a computer solution of PIRK (Ref. 15) with the lowest order optical potential. The solid curve shows the resulting calculation. Consideration of $\delta'(b)$ leads to a systematic improvement and it is seen that the simple theory does a very good job in reproducing the qualitative features of the experimental results. Quantitative agreement is also quite good.

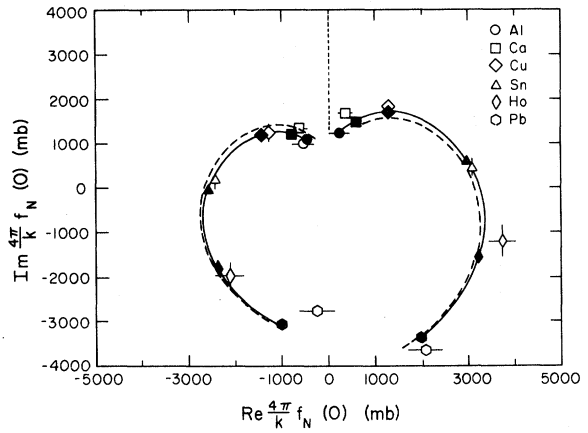

FIG. 8. Comparison of $(4\pi/k)f_N(0)$ with simple absorption model calculations for 165 MeV pions. Measured data points are represented by the open symbols while curves are used to represent different approximations in the absorption model calculations. The dotted curve represents a model for which the Coulomb phase was set equal to zero and for which $f_N(0)$ is purely imaginary. The dashed curve gives the results obtained when the point Coulomb phase are included. The solid line includes the additional effects arising from the finite extent of the charge distribution and the real part of the optical potential. The closed symbols give theoretical values of $(4\pi/k)f_N(0)$ corresponding to the targets measured in this experiment. For clarity, theoretical points are given only for the solid curve.

VI. COMPARISON WITH OTHER EXPERIMENTS

Because of difficulties associated with the Coulomb-nuclear interference term, few total pion nucleus cross section measurements on high-Z nuclei exist in the energy range covered in this experiment. Pion-nucleus total cross sections for π^+ and π^- mesons have been obtained by Carroll *et al.*[28] using standard transmission techniques. Measurements were made of partial cross sections for a number of nuclei including Al, Sn, and Pb in the energy range of 65–320 MeV. The results given in Sec. IV cannot be compared directly to the results reported by Carroll *et al.* since different quantities were reported. We did, however, use our data to determine a removal cross section for Pb and Al in order that some comparison might be made. The removal cross section was found by means of a third-order polynomial extrapolation of partial cross section data from which both the pure Coulomb and Coulomb-nuclear interference (CNI) contribution had been removed. The Kisslinger optical model was used for evaluation of the Coulomb-nuclear interference term.

Our results for σ_R are subject to all the uncertainties of the CNI subtraction described below. We found the agreement between our results and those reported by Carroll to be fairly good for Al at 215 MeV but poorer for lead at 115 MeV. The present experiment gives for π^+ on Al $\sigma_R=1054\pm13$ mb at 215 MeV and for Pb $\sigma_R=3407\pm131$ mb at 115

MeV. This is to be compared to Ref. 28, where for π^+ on Al $\sigma_R = 1060 \pm 27$ mb at 207 MeV and for Pb $\sigma_R = 4040 \pm 300$ mb at 117 MeV. Differences between the two sets of data for Pb could be statistical or explained in terms of the multiple scattering and pion decay corrections which were made to the raw data. The targets used by Carroll were approximately five times as thick as those used in this experiment.

Elastic scattering data on Pb at 162 MeV have been evaluated for $f_N(0)$ by Devereux[29] giving values of $(4\pi/k)f'_N(0)$ equal to $-1621-i2506$ mb for π^+ on Pb and $1703-i3644$ mb for π^- on Pb. An extended charge distribution and nonrelativistic phase shifts were used in determining the Coulomb amplitude. If the results of this experiment are adjusted to give forward scattering amplitudes which correspond to use of nonrelativistic phase shifts and an extended charge distribution, one obtains $-1550 \pm 387 - i(2598 \pm 108)$ mb for π^+ on Pb at 165 MeV. The corresponding values for π^- on Pb are $3072 \pm 368 - i(3805 \pm 146)$ mb. Good agreement is observed with Devereux for the π^+ data but the real part of the π^- data differs by almost four standard deviations. It should be noted that it was necessary for Devereux to renormalize the elastic scattering data to produce a good fit. It is uncertain what effect this might have upon the result.

VII. SUMMARY OF RESULTS

We have obtained experimental values for the Coulomb-distorted nuclear forward scattering amplitude $f_N(0)$ for both π^+ and π^- mesons on Al, Cu, ^{40}Ca, Sn, Ho, and Pb in the energy range 114 to 215 MeV. The data should be useful in the evaluation of various models for the pion-nucleus interaction since the method which was used for the analysis of the data enables one to extract both the real and the imaginary parts of a well-defined forward scattering amplitude. The model-dependence is much less than that which has previously been observed in attenuation experiments involving pion-scattering on heavy nuclei.[28] The systematic uncertainties due to the residual model dependence for the two models which were tried appear to be slightly greater than the statistical errors for lower energies and less than the statistical errors for higher energies.

Some insight into the nature of $f_N(0)$ has been obtained by comparing experimental values with theoretical values calculated from a simple absorption model. These calculations demonstrate that the major part of the observed rotation of $f_N(0)$ in the Argand plane can be attributed to the Coulomb phase. The amount of rotation increases with Z and explains the negative values of $\mathrm{Im}[(4\pi/k)f_N(0)]$ which are observed for scattering of pions on Pb, Ho, and Sn.

Previously published results are in general agreement with those of this experiment. The resonance energy for ^{40}Ca of 154 ± 10 MeV is consistent with the resonance energies of other elements.

ACKNOWLEDGMENTS

We would like to express our appreciation to the staff of the LAMPF accelerator for their cooperation and assistance during all phases of the experiment. This research was supported in part by grants from the U.S. Department of Energy.

APPENDIX

Following the method given in Ref. 5, Eq. (5) is rewritten in terms of integrals over the solid angle subtended by each counter

$$\sigma_N(\Omega) = \sigma_N + \sum_n D_n \Omega^n - \int_0^\Omega |f_N|^2 d\Omega' - 2\,\mathrm{Re}\int_0^\Omega f_C^* f_N d\Omega' \,. \tag{A1}$$

The first integral in (A1) can be incorporated into the power series in Ω by assuming that f_N can also be written in terms of a Taylor series about $\Omega = 0$. The last integral is evaluated by using an approximation for the relativistic point Coulomb amplitude found in Ref. 17:

$$f_C^*(\Omega) = -\frac{\eta}{2k} e^{-2i\sigma_0} \sum_{j=0}^{3} A_j^* \left[\frac{\Omega}{4\pi}\right]^{(j/2)-1+i\eta} . \tag{A2}$$

The use of this equation, along with the Taylor series expansion of f_N, gives

$$\int_0^{\Omega} f_C^* f_N d\Omega' = \frac{2\pi}{k} f_N(0) \left\{ [i(e^{-2i\sigma_{\gamma 0}} - 1)] + \eta \sum_{j=0}^{3} A_j^* \left[\frac{e^{-2i\sigma_0}}{\frac{j}{2} + i\eta} - \frac{e^{iW} \left[\frac{\Omega}{4\pi} \right]^{j/2}}{\frac{j}{2} + i\eta} \right] \right\} \tag{A3}$$

$$- \frac{2\pi\eta}{k} \sum_{n=1} E_n \sum_{j=0}^{3} A_j^* \frac{(4\pi)^n \left[\frac{\Omega}{4\pi} \right]^{(j/2)+n} e^{iW}}{\frac{j}{2} + n + i\eta} .$$

As a result,

$$\sigma_N(\Omega) = \frac{4\pi}{k} f_N^I G(\Omega) + \frac{4\pi}{k} f_N^R H(\Omega) + \sum_{n=1} K_n \Omega^n + \sum_{n=0} B_n \Omega^{1+(n/2)} \cos W + \sum_{n=0} C_n \Omega^{1+(n/2)} \sin W , \tag{A4}$$

where

$$G(\Omega) = \mathrm{Re}(e^{-2i\sigma_{\gamma 0}}) - \eta \{ A^R \sin 2\sigma_0 - A^I \cos 2\sigma_0 + F^I(\Omega) \cos W + F^R(\Omega) \sin W \} \tag{A5a}$$

and

$$H(\Omega) = \mathrm{Im}(e^{-2i\sigma_{\gamma 0}}) - \eta \{ A^R \cos 2\sigma_0 + A^I \sin 2\sigma_0 - F^R(\Omega) \cos W + F^I(\Omega) \sin W \} . \tag{A5b}$$

The K_n's are constants which are obtained by the combining of the coefficients which multiply Ω^n. The A's and F's are defined according to

$$\sum_{j=0}^{3} \frac{A_j^*}{\frac{j}{2} + i\eta} \equiv A^R + iA^I , \tag{A6a}$$

$$\sum_{j=0}^{3} \frac{A_j^* \left[\frac{\Omega}{4} \right]^{j/2}}{\frac{j}{2} + i\eta} \equiv F^R(\Omega) + iF^I(\Omega) . \tag{A6b}$$

---

*Present address: Massachusetts Institute of Technology, Cambridge, MA 02139.

†Present address: Laboratorium für Hochenergiephysic Eidgenossische Technische Hochschule Zürich, CH-5234 Villigen, Switzerland.

‡Present address: Lawrence Livermore Laboratory, Livermore, CA 94550.

§Present address: Indiana University, Bloomington, IN 47405.

[1]See, for example, B. W. Allardyce *et al.*, Nucl. Phys. A209, 1 (1973).

[2]F. Binion *et al.*, Nucl. Phys. B33, 42 (1971).

[3]T. E. O. Ericson and M. P. Locher, Nucl. Phys. A148, 1 (1970).

[4]J. P. Albanese *et al.*, Nucl. Phys. A350, 301 (1980).

[5]M. D. Cooper and M. B. Johnson, Nucl. Phys. A260, 352 (1976).

[6]L. I. Schiff, *Quantum Mechanics,* 3rd ed. (McGraw-Hill, New York, 1968).

[7]M. D. Cooper, M. B. Johnson, and G. B. West, Nucl. Phys. A292, 350 (1977).

[8]R. L. Burman, R. L. Fulton, and M. Jakobson, Nucl. Instrum. Methods 131, 29 (1975).

[9]J. Litt and R. Meunier, Annu. Rev. Nucl. Sci. 23, 1 (1973).

[10]M. D. Cooper, Los Alamos Scientific Laboratory Report LA-55-29-MS, 1974.

[11]G. Giacomelli, in *Progress in Nuclear Physics,* edited by D. M. Brink and J. H. Mulvey (Pergamon, New York, 1970), Vol. 12.

[12]K. F. Johnson, Ph.D. dissertation, New Mexico State University, 1976.

[13]R. H. Jeppesen, Ph.D. dissertation, New Mexico State University, 1979.
[14]Monte Carlo program DEC written by L. Knutson.
[15]R. A. Eisenstein and G. A. Miller, Comput. Phys. Commun. 8, 130 (1974).
[16]A. S. Clough *et al.*, Phys. Lett. 43B, 476 (1973).
[17]M. D. Cooper, R. H. Jeppesen, and M. B. Johnson, Phys. Rev. C 20, 696 (1979).
[18]L. S. Kisslinger, Phys. Rev. 98, 761 (1955).
[19]See, for example, M. Sternheim and R. Silbar, Annu. Rev. Nucl. Sci. 24, 249 (1974).
[20]P. R. Bevington, *Data Reduction and Error Analysis for the Physical Sciences* (McGraw-Hill, New York, 1969).
[21]H. A. Bethe, Ann. Phys. (N.Y.) 3, 1960 (1958).
[22]G. B. West and D. R. Yennie, Phys. Rev. 172, 1413 (1968).
[23]J.-F. Germond and M. B. Johnson, *Proceedings of the Eighth International Conference on High Energy Physics and Nuclear Structure, Vancouver,* edited by D. F. Measday and A. W. Thomas (North-Holland, Amsterdam, 1980).
[24]J.-F. Germond and C. Wilkin, Phys. Lett. 68B, 229 (1977).
[25]J.-F. Germond and M. B. Johnson, Phys. Rev. C 22, 1622 (1980).
[26]J.-F. Germond and C. Wilkin, Ann. Phys. (N.Y.) 121, 285 (1979).
[27]M. B. Johnson and H. A. Bethe, Comments Nucl. Part. Phys. 8, 75 (1978).
[28]A. S. Carroll *et al.*, Phys. Rev. C 14, 635 (1976).
[29]M. J. Devereux, Ph.D. dissertation, New Mexico State University, 1979.